Electronic supplementary information (ESI)

Photoactive conducting polymers with light-driven conductivity modulation: dual functionality for simple circuits

*Seung-Chul Lee, Suck-Hyun Lee and O-Pil Kwon**

Device Structures of Conventional Photoactive LCM Devices

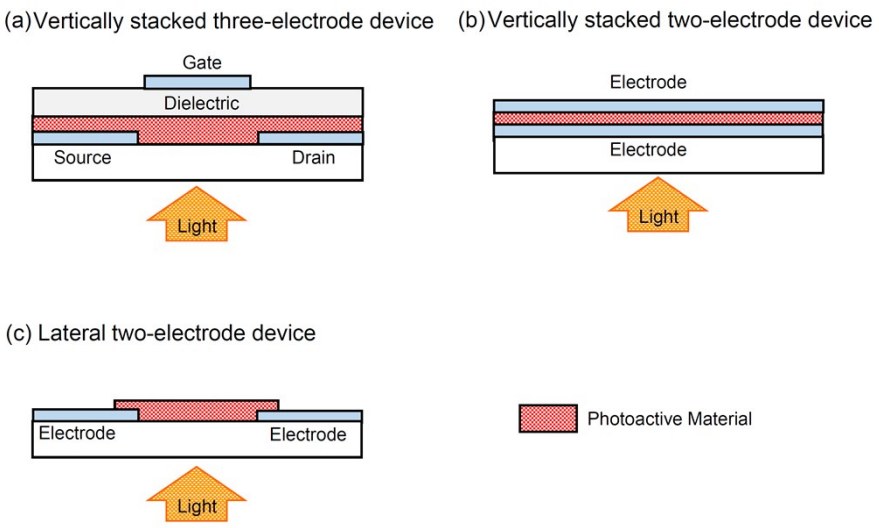

Fig. S1 Conventional light-driven conductivity modulation (LCM) devices with small gap between electrodes (less than a few micrometers): (a) vertically stacked multilayer three-electrode device with the thin film transistor (TFT) structure, (b) vertically stacked two-electrode device with the organic photovoltaic (OPV) cell structure, and (c) lateral two-electrode device.

Photostability of PANI-CSA film

The photochemical stability of PANI-CSA films is measured using UV-vis-NIR absorption spectroscopy. The UV-vis-NIR absorption spectrum of PANI-CSA film is measured after pump beam illumination at the wavelength of λ_{pump} = 514 nm with an intensity of I_{pump} = 183 mW/cm^2. Various illumination times (1, 2, 4, and 6 h) are tested for photostability measurement. As shown in Figure S2, the UV-vis-NIR absorption spectrum of the PANI-CSA film after illumination for 6 h is nearly identical to that of PANI-CSA film without illumination. Therefore, the PANI-CSA film exhibits highly stable photochemical stability at a wavelength of 514 nm.

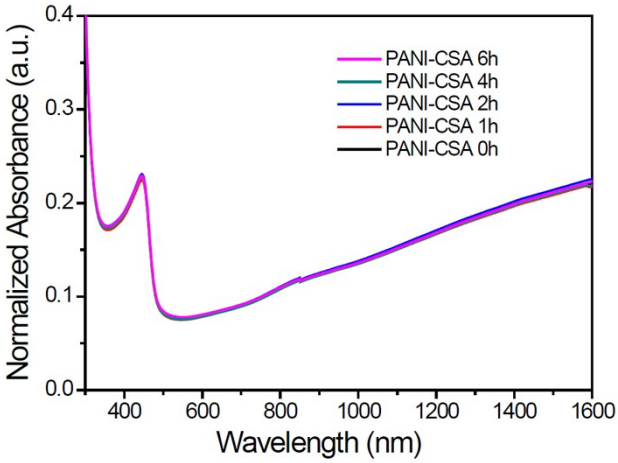

Fig. S2 Photochemical stability of PANI-CSA film: UV-vis-NIR absorption spectra of PANI-CSA film with pump beam illumination at λ_{pump} = 514 nm (I_{pump} = 183 mW/cm^2) with various illumination times: 0, 1, 2, 4, and 6 h.

Intermolecular Interactions in Polyaniline Films

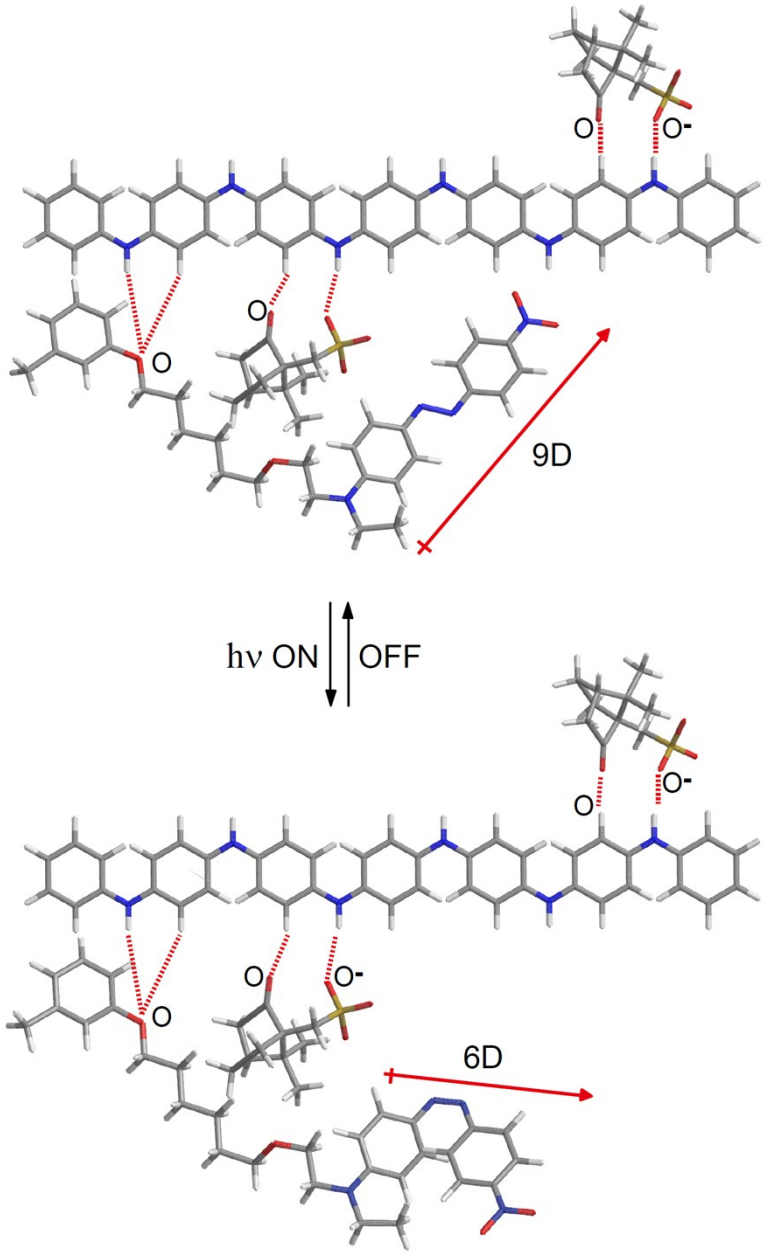

Fig. S3 Schematic illustration of suggested intermolecular interactions in photoactive polyaniline films. The dotted lines present hydrogen bonds between protons of the polyaniline backbone and (partially) negatively charged oxygen atoms.

Response Rates of LCM Behavior

To investigate the dynamics of growth and decay of light-driven conductivity modulation, growth response rates (τ_g) and decay response rates (τ_g) are evaluated. The growth response rate (τ_g) is obtained by fitting the growth of the amplitude of conductivity modulation ($-\Delta\delta$) to an equation with double-exponential time dependence: $y = y_0 + A_1 e^{x/\tau_1} + A_2 e^{x/\tau_2}$, whereas the decay response rate (τ_d) is obtained by fitting the decay of the amplitude of conductivity modulation ($-\Delta\delta$) to an equation with double-exponential time dependence: $y = y_0 + A_1 e^{-x/\tau_1} + A_2 e^{-x/\tau_2}$. The normalized conductivity modulation curves of PNA10, PNA20, and PNA30 films are superimposed in Figure S4. The normalized conductivity modulation curves of PNA20 films with different pump intensity are superimposed as shown in Figure S5. As a result, the growth response rate (τ_g) and decay response rate (τ_d) exhibit no dependence on concentration of ENA photoactive compound or pump intensity. Therefore, to evaluate the growth response rate (τ_g) and decay response rate (τ_d) as listed in Table S1, the corresponding values in Table S2-S6 are averaged. For reliable fitting data, conductivity modulation data with a relatively large amplitude at a pump intensity of over I_{pump} = 40 mW/cm^2 are used. To eliminate hysteresis of cycles, the first and third ON-OFF cycles in Figure 5a and 5b are used (see Table S3-S6).

Table S1. The response rates for growth and decay dynamics under conductivity modulation, which are the average values of response rates in Table S2-S6.

ON (growth)				OFF (decay)			
$A_{g,1}$	$\tau_{g,1}$	$A_{g,2}$	$\tau_{g,2}$	$A_{d,1}$	$\tau_{d,1}$	$A_{d,2}$	$\tau_{d,2}$
0.43±0.11	3.1±0.8	0.41±0.12	25.0 ± 5.8	0.39±0.11	3.1±0.6	0.38±0.11	23.0±2.6

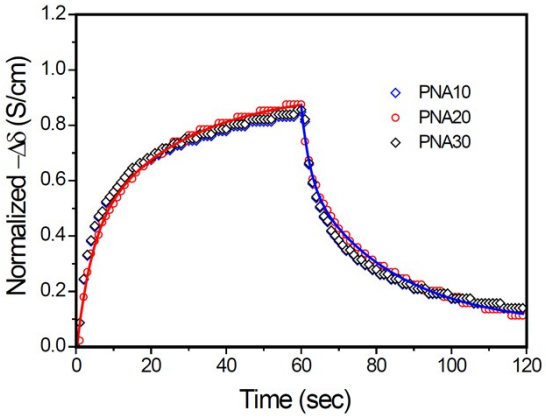

Fig. S4 Normalized amplitude of conductivity modulation (-$\Delta\delta$) of PNA10, PNA20, and PNA30 films, which are normalized from the first ON-OFF cycle in Figure 3c (parallel configuration, λ_{pump} = 514 nm, I_{pump} = 133 mW/cm^2). The solid lines present the fitting curves of PNA20 film with double-exponential growths and decays, for example.

Table S2. The response rates in growth and decay dynamics of conductivity modulation for Fig. S4.

	ON (growth)					OFF (decay)				
	y_0	$A_{g,1}$	$\tau_{g,1}$	$A_{g,2}$	$\tau_{g,2}$	y_0	$A_{d,1}$	$\tau_{d,1}$	$A_{d,2}$	$\tau_{d,2}$
PNA10	0.88	0.46	3.19	0.44	26.55	0.10	0.39	3.42	0.38	24.60
PNA20	0.93	0.42	3.93	0.54	26.27	0.07	0.53	2.38	0.26	24.16
PNA30	0.89	0.44	3.19	0.47	26.6	0.10	0.39	3.42	0.39	24.60

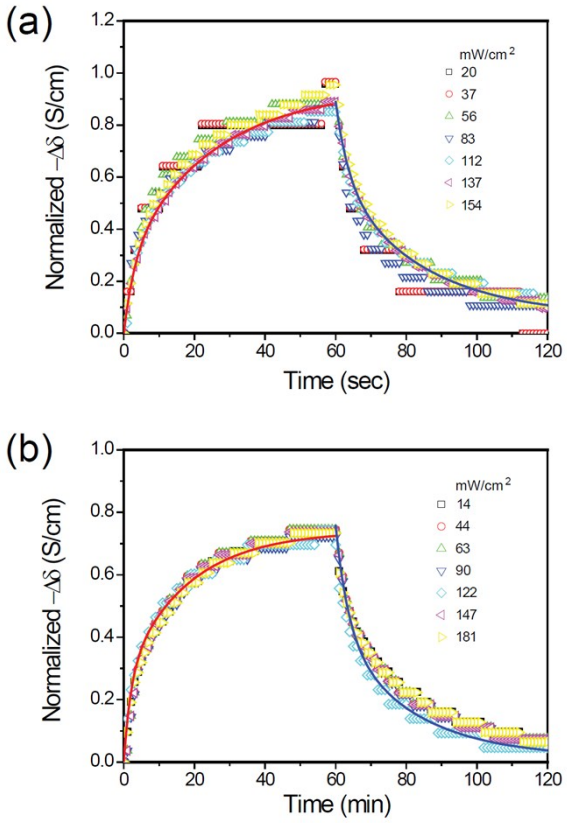

Fig. S5 Normalized amplitude of conductivity modulation (-$\Delta\delta$) of PNA20, pumped at λ_{pump} = 514 nm with various pump intensities in (a) parallel and (b) perpendicular configurations, which are normalized from the first ON-OFF cycle in Figure 5a and 5b, respectively. For these examples, the solid lines present the fitting curves of (a) 137 mW/cm^2 for parallel configurations and (b) 122 mW/cm^2 for perpendicular configurations.

Table S3. The response rates in growth and decay dynamics of conductivity modulation with parallel configuration for Fig. S5a (the first ON-OFF cycle in Fig. 5a).

I_{pump}	ON (growth)					OFF (decay)				
(mW/cm^2)	y_0	$A_{g,1}$	$\tau_{g,1}$	$A_{g,2}$	$\tau_{g,2}$	y_0	$A_{d,1}$	$\tau_{d,1}$	$A_{d,2}$	$\tau_{d,2}$
56	0.94	0.45	3.80	0.52	25.02	0.08	0.48	3.37	0.32	23.83
83	0.92	0.37	2.47	0.56	28.12	0.08	0.32	2.28	0.47	16.80
112	0.92	0.58	3.48	0.36	26.93	0.09	0.28	3.21	0.49	24.40
137	0.94	0.28	3.09	0.67	24.71	0.06	0.29	3.72	0.53	24.09
154	1.09	0.65	4.29	0.43	40.65	0.07	0.57	3.51	0.33	23.40

Table S4. The response rates in growth and decay dynamics of conductivity modulation with parallel configuration for the third ON-OFF cycle in Fig. 5a.

I_{pump}	ON (growth)					OFF (decay)				
(mW/cm^2)	y_0	$A_{g,1}$	$\tau_{g,1}$	$A_{g,2}$	$\tau_{g,2}$	y_0	$A_{d,1}$	$\tau_{d,1}$	$A_{d,2}$	$\tau_{d,2}$
56	1.00	0.51	2.10	0.33	19.21	0.17	0.56	1.72	0.28	17.83
83	1.01	0.53	2.51	0.37	21.55	0.12	0.31	2.99	0.53	22.78
112	0.92	0.49	2.54	0.29	20.95	0.11	0.28	3.94	0.49	27.50
137	0.95	0.47	5.18	0.35	31.52	0.08	0.56	3.33	0.26	22.11
154	0.83	0.60	2.61	0.24	18.96	-0.03	0.31	4.23	0.53	26.43

Table S5. The response rates in growth and decay dynamics of conductivity modulation with perpendicular configuration for Fig. S5b (the first ON-OFF cycle in Fig. 5b).

I_{pump}	ON (growth)					OFF (decay)				
(mW/cm^2)	y_0	$A_{g,1}$	$\tau_{g,1}$	$A_{g,2}$	$\tau_{g,2}$	y_0	$A_{d,1}$	$\tau_{d,1}$	$A_{d,2}$	$\tau_{d,2}$
44	0.77	0.31	3.61	0.49	19.56	0.04	0.23	2.71	0.49	20.46
63	0.77	0.31	3.61	0.49	19.56	0.04	0.23	2.71	0.48	20.46
90	0.75	0.30	3.61	0.47	19.56	0.04	0.47	2.71	0.23	20.46
122	0.74	0.27	2.02	0.47	17.79	0.02	0.41	3.61	0.33	20.90
147	0.76	0.48	3.61	0.31	19.56	0.04	0.47	2.71	0.23	20.46
181	0.76	0.54	2.11	0.22	18.20	0.03	0.21	2.09	0.48	22.68

Table S6. The response rates in growth and decay dynamics of conductivity modulation with perpendicular configuration for the third ON-OFF cycle in Fig. 5b.

I_{pump}	ON (growth)					OFF (decay)				
(mW/cm^2)	y_0	$A_{g,1}$	$\tau_{g,1}$	$A_{g,2}$	$\tau_{g,2}$	y_0	$A_{d,1}$	$\tau_{d,1}$	$A_{d,2}$	$\tau_{d,2}$
44	0.87	0.31	3.75	0.49	31.68	0.08	0.45	3.24	0.28	25.00
63	0.87	0.31	3.75	0.49	31.68	0.08	0.45	3.24	0.25	25.00
90	0.85	0.47	3.75	0.30	31.68	0.08	0.27	3.24	0.44	25.00
122	0.89	0.28	2.01	0.55	24.12	0.08	0.29	2.44	0.48	21.21
147	0.87	0.49	3.75	0.31	31.68	0.08	0.45	3.24	0.28	25.00
181	0.83	0.53	1.89	0.20	23.30	0.10	0.43	3.05	0.26	24.93